# Influence of *cis* Double Bonds in the *sn*-2 Acyl Chain of Phosphatidylethanolamine on the Gel-to-Liquid Crystalline Phase Transition

Guoquan Wang, Shusen Li, Hai-nan Lin, and C. Huang
Department of Biochemistry, Health Sciences Center, University of Virginia, Charlottesville, Virginia 22908 USA

ABSTRACT We have semisynthesized 19 species of mixed-chain phosphatidylethanolamines (PEs) in which the *sn*-1 acyl chain is derived from saturated fatty acids with varying chain lengths and the *sn*-2 acyl chain has different chain lengths but contains 0, 1, and 2 *cis* double bond(s). The gel-to-liquid crystalline phase transition temperatures ($T_m$) of lipid bilayers prepared from these 19 mixed-chain PEs were determined calorimetrically. When the $T_m$ values are compared with those of saturated and monounsaturated counterparts, a common $T_m$ profile is observed in the plot of $T_m$ versus the number of *cis* double bonds. Specifically, a marked stepwise decrease in $T_m$ is detected as the number of *cis* double bonds in the *sn*-2 acyl chain of the mixed-chain PE is successively increased from 0 to 1 and then to 2. The large $T_m$-lowering effect of the acyl chain unsaturation can be attributed to the increase in Gibbs free energy of the gel-state bilayer as a result of weaker lateral chain-chain interactions. In addition, we have applied molecular mechanics calculations to simulate the molecular structure of dienoic mixed-chain C(*X*):C(*Y*:2$\Delta^{n,n+3}$)PE in the gel-state bilayer, thus enabling the three independent structural parameters (*N*, $\Delta C$, and LS) to be calculated in terms of *X*, *Y*, and *n*, which are intrinsic quantities of C(*X*):C(*Y*:2$\Delta^{n,n+3}$)PE. When the $T_m$ values and the corresponding *N* and $\Delta C$ values of all dienoic mixed-chain PEs under study are first codified and then analyzed statistically by multiple regressions, the dependence of $T_m$ on the structural parameters can be described quantitatively by a simple and general equation. The physical meaning and the usefulness of this simple and general equation are explained.

## INTRODUCTION

Phosphatidylcholines (PCs) and phosphatidylethanolamines (PEs) are quantitatively the most important phospholipid species found in a wide variety of biological membranes, in which these zwitterionic phospholipid molecules self-assemble into the well-known organized structure called the lipid bilayer. Because of this, the physicochemical properties of bilayers composed of PC or PE containing both saturated or both unsaturated acyl chains have been studied exhaustively. In biological membranes, PC and PE are typically of a mixed acyl chain variety, in which the *sn*-1 acyl chain is often derived from a saturated fatty acid with varying chain lengths, whereas the *sn*-2 acyl chain is usually an unsaturated fatty acid of different chain lengths containing a single *cis* double bond or two to six methylene-interrupted *cis* double bonds (Kunau, 1976). In the literature, however, most elegant studies on mixed-chain phospholipid bilayers have been concerned primarily with PC (Barton and Gunstone, 1975; Litman et al., 1991; Hernandez-Borrell and Keough, 1993; Niebylski and Salem, 1994). Our current knowledge about the packing structure and chain melting behavior of mixed-chain PE with *sn*-1 saturated/*sn*-2 unsaturated acyl chains remains incomplete.

Recently we began a project of studying the gel-to-liquid crystalline phase transition behavior of a large number of homologous series of monounsaturated PC and PE with *sn*-1 saturated/*sn*-2 *cis* monoenoic acyl chains by high-resolution differential scanning calorimetry (DSC). The calorimetric results were then analyzed using the molecular structures of these monounsaturated phospholipids obtained with computer-based molecular mechanics (MM) simulations. The combined approach of DSC and MM simulation studies provided valuable information relating the structure and chain melting behavior of monoenoic phospholipids in the bilayer (Z-q. Wang et al., 1994, 1995; G. Wang et al., 1995; Huang et al., 1996). For instance, the position of a single *cis* double bond ($\Delta^n$) in the *sn*-2 acyl chain can exert a characteristic influence on the gel-to-liquid crystalline phase transition temperature ($T_m$) for bilayers composed of either monoenoic PC or PE. Specifically, in the plot of $T_m$ versus $\Delta^n$, an inverted bell-shaped $T_m$ profile is observed,

*Received for publication 21 February 1997 and in final form 8 April 1997.*

Address reprint requests to Dr. Ching-hsien Huang, Box 440, Department of Biochemistry, University of Virginia School of Medicine, Charlottesville, VA 22908. Tel.: 804-924-5010; Fax: 804-924-5069; E-mail: ch9t@virginia.edu.

*Abbreviations used:* C(*X*):C(*Y*)PE refers to saturated phosphatidylethanolamine (PE) having *X* and *Y* carbon atoms in the *sn*-1 and *sn*-2 acyl chains, respectively. C(*X*):C(*Y*:1$\Delta^n$)PE refers to monounsaturated PE. The shorthand notation C(*X*) preceding the first colon indicates the total number of carbon atoms, *X*, in the *sn*-1 acyl chain, whereas the other, C(*Y*), succeeding the first colon represents the total number of carbons in the *sn*-2 acyl chain. The number 1 succeeding the second colon in the parentheses indicates that a single *cis* double bond is present in the *sn*-2 acyl chain, whereas $\Delta^n$ indicates that the single *cis* double bond is located at the *n*th carbon from the carboxyl end. Similarly, C(*X*):C(*Y*:2$\Delta^{n,n+3}$)PE designates a mixed-chain PE with a saturated *sn*-1 acyl chain and a dienoic *sn*-2 acyl chain in which two methylene-interrupted *cis* double bonds are at the *n* and (*n* + 3) carbon atoms from the carboxyl end. C(*X*):C(*Y*:2$\omega$6)PE designates the mixed-chain PE in which the *sn*-1 acyl chain has *X* carbon atoms and the unsaturated *sn*-2 acyl chain has *Y* carbon atoms. Furthermore, the notation 2$\omega$6 in the second set of parentheses indicates that there are two methylene-interrupted *cis* double bonds, and the *cis* double bond that is nearest the methyl end ($\omega$) is positioned at the sixth carbon atom counting from the methyl end of the *sn*-2 acyl chain.



0006-3495/97/07/283/10 $2.00

and the minimum $T_m$ occurs when the single *cis* double bond is positioned near the center of the linear segment of the *sn*-2 acyl chain. A molecular model for the monoenoic phospholipid constructed on the basis of experimental and computational data has been successfully used as a framework to interpret the characteristic dependence of $T_m$ on the position of $\Delta^n$ for monoenoic phospholipids (G. Wang et al., 1995).

Now, in an attempt to broaden our understanding of the structures and packing properties of various naturally occurring phospholipids, we extend our earlier work and focus our attention in this study on PE molecules with two *cis* double bonds in their *sn*-2 acyl chains. In particular, we have semisynthesized two mixed-chain PEs with both saturated acyl chains, two species of monoenoic PE with the *cis* double bond located in the *sn*-2 acyl chain, and 15 species of dienoic omega-6 PE with the two methylene-interrupted *cis* double bonds located in the *sn*-2 acyl chain. The molecular structure of each of these 15 species of C(*X*):C(*Y*:2$\omega$6)PE in the gel-state bilayer is uniquely characterized by three independent structural parameters ($\Delta C$, LS, and *N*) obtained with molecular mechanics simulations. In addition, the gel-to-liquid crystalline phase transition behavior of the bilayer composed of each of the semisynthesized mixed-chain PE species has been investigated by high-resolution DSC. When the $T_m$ values of two dienoic PEs, C(18):C(20:2$\Delta^{11,14}$)PE and C(20):C(18:2$\Delta^{9,12}$)PE, are compared with those of their saturated and monounsaturated counterparts, a marked decrease in $T_m$ for bilayers composed of dienoic PE is detected in each of the two series. Interestingly, it is also demonstrated in this work that a delicate balance between the two structural parameters (*N* and $\Delta C$) underlying the molecular species of C(*X*):C(*Y*:2$\omega$6)PE in the gel-state bilayer determines the unique $T_m$ value of each of the 15 lipid species under study. Hence a simple and general equation is derived that describes the dependence of $T_m$ for bilayers composed of dienoic $\omega$6PE on the two structural parameters (*N* and $\Delta C$).

## MATERIALS AND METHODS

### Semisynthesis of phosphatidylethanolamines

In this study, 19 molecular species of PE were semisynthesized. Two of them, C(18):C(20)PE and C(20):C(18)PE, were a pair of positional isomers, belonging to the class of saturated mixed-chain PEs. A second pair was monoenoic PE: C(18):C(20:1$\Delta^{11}$)PE and C(20):C(18:1$\Delta^{9}$)PE. The rest was a class of omega-6 PEs with *sn*-1 saturated/*sn*-2 diunsaturated acyl chains, C(*X*):C(*Y*:2$\omega$6)PE, which includes three series of a total of 15 lipid species as follows: C(*X*):C(18:2$\Delta^{9,12}$)PE, C(*X*):C(20:2$\Delta^{11,14}$)PE, and C(*X*):C(22:2$\Delta^{13,16}$)PE, where $X$ = 16, 18, 20, 22, and 24, indicating the total number of carbons in the *sn*-1 acyl chain. Initially, 19 molecular species of the corresponding PC were semisynthesized and purified by established procedures (Lin et al., 1990), with a modified condition that all procedures were carried out as far as possible in an $O_2$-free, $N_2$ atmosphere to minimize autoxidation. This precaution was also taken for the rest of the PE synthesis. The purified PCs (purity greater than 98%) were then converted to PEs by transphosphatidylation with phospholipase D in the presence of excess amounts of ethanolamine hydrochloride, at pH 5.6, according to the procedure of Comfurius and Zwall (1977) as previously published (Xu et al., 1988). However, in the case of C(18):C(20)PC and C(20):C(18)PC, which have high phase transition temperatures, the transphosphatidylation was carried out in the presence of sodium dodecyl sulfate to ensure the complete conversion of PC to PE by phospholipase D (Mason and Stephenson, 1990). The products were purified and separated by silica gel column chromatography, with which a mixture of $CHCl_3$/$CH_3OH$/5%$NH_4OH$ (175:35:4, v/v/v) was used to elute the lipids off the column. The purity of PE in the fractionated eluate was examined by thin-layer chromatography in $CHCl_3$/$CH_3OH$/5% $NH_4OH$ (65/30/5, v/v/v). Only a single spot was observed for each of the PEs synthesized, after ~1 $\mu$mol per sample was loaded on the thin-layer plate. Possible oxidation of the unsaturated fatty acyl chain in all synthesized phosphatidylethanolamines was checked spectroscopically at 234 nm (MacGee, 1959; Klein, 1970), and results indicate that most synthesized PE has only ~1.5–2.5% oxidized.

All fatty acids used as the starting materials for phospholipid semisynthesis were supplied by Nu Chek Prep (Elysian, MN) or Sigma Chemical Co. (St. Louis, MO). The other starting materials, lysophosphatidylcholines, were purchased from Avanti Polar Lipids (Alabaster, AL). Phospholipase D, type I from cabbage, was obtained from Sigma. All reagents and organic solvents were of reagent and spectroscopic grades, respectively.

### Molecular mechanics simulations

The computer station used was either an IBM RS/6000 or a Silicon Graphics/Indigo$^2$. The software for MM calculations was Allinger's MM3(92) force field supplied by Quantum Chemistry Program Exchange at the Chemistry Department, Indiana University. The output of MM calculations obtained with Allinger's MM3 program was entered into either HyperChem 4.5 or HyperChem 4.0 software (Hyper Cube, Waterloo, Canada) for molecular graphics visualizations on a Silicon Graphics/Indigo$^2$ or Pentium P5–200 platform. Details of the procedure of obtaining the energy-minimized structure and its steric energy for dienoic PE were identical to those developed in this laboratory for monoenoic PC as described elsewhere (G. Wang et al., 1995; Li and Huang, 1996; Li et al., 1996).

### High-resolution DSC measurements

The lipid samples were prepared according to established procedures (Huang et al., 1994). Initially, aqueous buffer solution (50 mM NaCl, 1 mM EDTA, 5 mM phosphate buffer, pH 7.4, and 0.02 mg/ml $NaN_3$) was added to lyophilized lipid powder to give a total lipid concentration of 3.5–4.5 mM. However, for dienoic lipid-containing buffer, the chelator EDTA (1 mM) was replaced by diethylenetriaminepentaacetic acid (0.25 mM). The exact lipid concentration was determined by phosphorus analysis. Before the first DSC scan, each lipid sample was kept in the sample cell within the calorimeter for 90 min at a temperature ~10°C below the estimated $T_m$. All DSC experiments were performed using a high-resolution MC-2 differential scanning microcalorimeter (Microcal, Northampton, MA). Each lipid sample was scanned at least three times at a scan rate of 15°C/h in the ascending temperature mode. To ascertain that the same thermal history pertained to all lipid samples, only the $T_m$ value from the second DSC heating scan was reported in this study. The third DSC heating scan served as an internal control to check whether the second DSC curve was reproducible. Details of the procedure for carrying out DSC experiments and for determining the values of the phase transition temperature ($T_m$) and enthalpy ($\Delta H$) were described in our earlier publication (Lin et al., 1990; Xu et al., 1988).

## RESULTS

### Molecular mechanics simulation studies

In naturally occurring fatty acids that contain polyunsaturated hydrocarbon chains, the *cis* double bonds ($\Delta$) are

usually methylene-interrupted; namely, two *cis* bonds are separated by a methylene unit. Because a *cis* double bond can bend an all-*trans* hydrocarbon chain with a 125.27° C-C=C angle (Pauling, 1960), one would expect that a long dienoic hydrocarbon chain with two methylene-interrupted *cis* double bonds may exhibit a highly curved semicircular topology. Recently it has been shown by MM simulations that a dienoic hydrocarbon chain can exhibit various kinked but fully extended conformations; most interestingly, these kinked conformations are energetically stable (Li and Huang, 1996). Specifically, the kinked conformation is characterized by a crankshaft-like topology, and the torsion angles of the two C-C single bonds located between the two *cis* double bonds in the (-CH=CH-$CH_2$-CH=CH-) segment adopt the *skew* (+) or *skew* (−) conformation (Li and Huang, 1996). The kinked dienoic hydrocarbon chain, with a $\Delta s^+ s^+ \Delta$ or $\Delta s^- s^- \Delta$ sequence, is able to pack very closely with neighboring all-*trans* saturated chains; hence, favorable lateral van der Waals contact interactions are ensured (Li and Huang, 1996). Here $s^+$ and $s^-$ represent *skew* (+) and *skew* (−) conformations, respectively; the *skew* (*s*) conformation of a single carbon-carbon bond has a torsion angle of 120° ± 30°; the superscripts in $s^+$ and $s^-$ are defined as (+) and (−) torsion angles. Based on these MM calculations, one can expect that when mixed-chain phospholipid molecules with *sn*-1 saturated/*sn*-2 dienoic acyl chains are packed in the gel-state bilayer at $T < T_m$, the *sn*-1 acyl chains, with all methylene units staggering regularly in a *trans* (. . . *ttt* . . . ) conformation, and the *sn*-2 acyl chains, with kinked ($\Delta s^+ s^+ \Delta$ or $\Delta s^- s^- \Delta$) conformations, are most likely to prevail in the bilayer structure (Li and Huang, 1996).

In this study, rotational isomers (or rotamers) of C(16):C(18:2$\Delta^{9,12}$)PE were initially constructed, and they were then subject to energy minimizations determined with Allinger's MM3 program. In particular, only the diglyceride moiety was allowed to undergo energy minimization, whereas the headgroup was fixed to have the same conformation as that of the C(12):C(12)PE determined in the presence of acetic acid by x-ray crystallography (Hitchcock et al., 1974). Initially, eight rotational isomers of the diglyceride moiety of C(16):C(18:2$\Delta^{9,12}$)PE were assigned. These rotamers were chosen because their *sn*-1 and *sn*-2 acyl chain axes were nearly parallel (Li and Huang, 1996); in addition, their *sn*-2 acyl chains contained no *gauche* bonds, so that no large energy expenditures were required for the formation of these rotamers. In these eight rotamers, all of the *sn*-1 acyl chains were assigned the same all-*trans* conformation. The *sn*-2 acyl chains of these rotamers, however, were assigned different conformations, each with a unique sequence. Specifically, the eight sequences in the *sn*-2 acyl chains at the kink or the core sequence ($\Delta s^+ s^+ \Delta$ or $\Delta s^- s^- \Delta$) were as follows: $s^-$(core)$s^-$, $s^+$(core)$s^-$, $s^-$(core)$s^+$, and $s^+$(core)$s^+$. The selection of *s* adjacent to the two ends of the core ($\Delta s^+ s^+ \Delta$ or $\Delta s^- s^- \Delta$) was based on the minimum steric energy of the *s* conformation as demonstrated by rotating from 180° to −180°, in 5° increments, about the C-C single bond adjacent to the core sequence, using MM calculations (Li and Huang, 1996).

Initially, each crude structure of the diglyceride moiety of C(16):C(18:2$\Delta^{9,12}$)PE rotamers was taken to be identical to that of the energy-minimized C(16):C(18:1$\Delta^9$)PE (Z-q. Wang et al., 1994), with the *sn*-2 acyl chain containing one of the eight sequences just discussed above. The torsion angles for *t*, Δ, and *s* were initially taken, before energy minimization, as 180° (or −180°), 0°, and 90°-150°, respectively. The various torsion angles of the headgroup structure of C(16):C(18:2$\Delta^{9,12}$)PE, as mentioned earlier, were fixed, having the same values as those of C(12):C(12)PE obtained crystallographically. The diglyceride moieties of the eight C(16):C(18:2$\Delta^{9,12}$)PE rotamers were then subjected to energy minimizations by MM calculations. The MM calculations can yield not only the energy-minimized structure of each rotamer, but also the steric energy ($E_s$) of the energy-minimized rotamer. The term $E_s$ calculated from Allinger's MM3 force field contains a combination of many energy terms, including bond stretching, angle bending, torsion, nonbonded van der Waals, dipole-dipole, charge-charge, stretching-bending, bending-torsion, and charge-dipole interaction energies (Allinger et al., 1989). Conceptually, the steric energy in molecular mechanics is analogous to the enthalpy in thermodynamics. Hence, the smaller the steric energy of the rotamer, the more stable the rotamer. The results of our MM calculations are presented in Table 1. The rotamer with a $s^- \Delta s^+ s^+ \Delta s^-$ sequence in the *sn*-2 acyl chain is energetically the most stable conformation (Table 1), and two projected views of the structure of the most stable rotamer are graphically presented in Fig. 1, *A* and *B*.

Before we specify the structural characteristics underlying the energy-minimized rotamers of C(16):C(18:2$\Delta^{9,12}$)PE as listed in Table 1, it is appropriate to mention first that an energy-minimized structure of the diglyceride moiety of C(16):C(18:2$\Delta^{9,12}$)PE has previously been proposed by Applegate and Glomset (1991), in which two *gauche*(−) bonds are introduced at the two ends of a $s^- \Delta s^- s^- \Delta s^-$ sequence in the *sn*-2 acyl chain. The computer-simulated PE molecule, constructed on the basis of

**TABLE 1 Energy-minimized conformations of C(16):C(18:2$\Delta^{9,12}$)PE rotamers obtained by MM simulations.**

| Sequence type | $\sigma_8$ | $\Delta^9$ | $\sigma_{10}$ | $\sigma_{11}$ | $\Delta^{12}$ | $\sigma_{13}$ | $E_s$ |
|---|---|---|---|---|---|---|---|
| $s^- \Delta s^+ s^+ \Delta s^-$ | −108.4 | 0.6 | 123.4 | 112.1 | 1.0 | −102.5 | −0.25 |
| $s^+ \Delta s^+ s^+ \Delta s^-$ | 109.7 | −1.0 | 86.3 | 87.4 | −0.1 | −118.4 | 0.08 |
| $s^- \Delta s^+ s^+ \Delta s^+$ | −120.2 | 0.3 | 115.0 | 90.0 | 0.8 | 115.8 | 0.14 |
| $s^+ \Delta s^+ s^+ \Delta s^+$ | 118.0 | 0.2 | 80.7 | 69.5 | 0.1 | 139.0 | 1.01 |
| $s^+ \Delta s^- s^- \Delta s^+$ | 118.7 | 0.1 | −119.7 | −117.6 | 0.1 | 117.9 | −0.08 |
| $s^+ \Delta s^- s^- \Delta s^-$ | 123.1 | 0.1 | −110.7 | −91.1 | −0.1 | −112.7 | 0.12 |
| $s^- \Delta s^- s^- \Delta s^+$ | −108.3 | 0.9 | −91.6 | −96.1 | 0.7 | 124.0 | 0.37 |
| $s^- \Delta s^- s^- \Delta s^-$ | −114.0 | 0.6 | −77.4 | −74.9 | −0.6 | −137.9 | 0.57 |

$\sigma_n$ and $\Delta^n$ refer to the torsion angles in degree for the single and *cis* double bonds, respectively, located at the C(*n*) position along the *sn*-2 acyl chain from the carboxyl end. $E_s$ is the steric energy in kcal/mol; the headgroup of the rotamer has a fixed conformation with torsion angles corresponding to those of C(12):C(12)PE, which were obtained crystallographically.

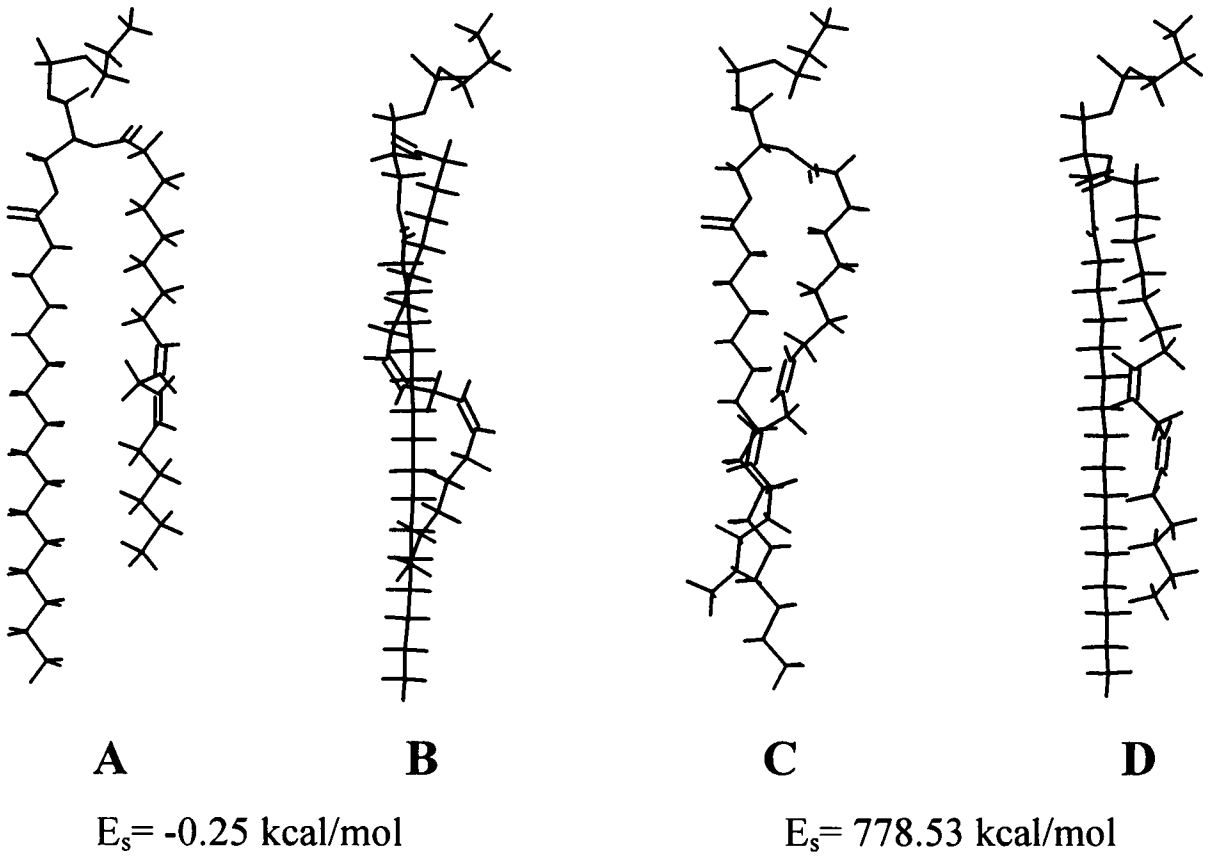


FIGURE 1 Molecular graphics representation of the energy-minimized structure of C(16):C(18:2$\Delta^{9,12}$)PE together with the calculated value of steric energy ($E_s$). (*A*) The low-energy rotamer in which the *sn*-2 acyl chain has a kink sequence of $s^-\Delta s^+s^+\Delta s^-$, with those torsion angles given in Table 1. The zigzag plane of the *sn*-1 acyl chain of this low-energy rotamer lies in the paper plane. (*B*) A different projected view of *A*, with the zigzag plane of the *sn*-1 acyl chain lying perpendicular to the paper plane and behind the kinked *sn*-2 acyl chain. (*C*) The *sn*-2 acyl chain has a kinked sequence of $g^-s^-\Delta s^-s^-\Delta s^-g^-$, and the lipid conformation is constructed based on the torsion angles given by Applegate and Glomset (1991). (*D*) A different projected view of *C*. Note that the two *cis* double-bond axes shown in *D* are oriented nearly parallel to the long-chain axis of the *sn*-1 acyl chain; however, the steric energy is extremely high.

published torsion angles by Applegate and Glomset (1991), is illustrated in two projected views as shown in Fig. 1, *C* and *D*. In one view, the two acyl chain axes are clearly seen to deviate significantly from the parallel packing (Fig. 1 *C*); the steric energy of this structural model ($g^-s^-\Delta s^-s^-\Delta s^-g^-$) is extremely high (778.53 kcal/mol) because of substantial repulsive interactions between the two acyl chains. The energy-minimized structure of the diglyceride moiety of C(16):C(18:2$\Delta^{9,12}$)PE proposed by Applegate and Glomset is thus considerably less stable than those proposed by this work as summarized in Table 1, including the one shown graphically in Fig. 1, *A* and *B*.

With the exception of the rotamer containing a sequence of $s^+\Delta s^+s^+\Delta s^+$, the steric energies of various rotamers of C(16):C(18:2$\Delta^{9,12}$)PE shown in Table 1 fall into a narrow range of −0.25 to +0.57 kcal/mol, suggesting that the C-C single bonds adjacent to the methylene-interrupted *cis* double bonds are remarkably flexible at room temperature. The one ($s^-\Delta s^+s^+\Delta s^-$) with the low energy (−0.25 kcal/mol), however, is present to a larger extent at lower temperatures. Several structural features are displayed by this low-energy rotamer of C(16):C(18:2$\Delta^{9,12}$)PE, as shown in Fig. 1, *A* and *B*. First, the zigzag planes of the two acyl chains are roughly parallel. This simulated feature is distinctly different from that of C(16):C(18:2$\Delta^{9,12}$)PC, which is characterized by two nearly perpendicular zigzag planes. Second, the MM simulated kink with a crankshaft-shaped topology is in excellent agreement with the experimentally determined chain motif obtained with single crystals of linoleic acid by x-ray diffraction (Ernst et al., 1979; Li and Huang, 1996). Specifically, in the kink region ($s^-\Delta s^+s^+\Delta s^-$), the two methylene-interrupted *cis* double bonds lie in two separate planes that are nearly perpendicular to each other; however, the two double-bond axes are parallel to each other. Moreover, the two double-bond axes are tilted relative to the direction of the long-chain axis of the *sn*-1 acyl chain (Fig. 1 *B*). In contrast, both double-bond directions are parallel to the long *sn*-1 acyl chain axis in the model structure ($g^-s^-\Delta s^-s^-\Delta s^-g^-$) of C(16):C(18:2$\Delta^{9,12}$)PE proposed by Applegate and Glomset (1991), as shown in Fig. 1 *D*. Third, the effective chain length of the kinked *sn*-2 acyl chain is shortened by about two C-C bond lengths along the long

chain axis in comparison with that of saturated *sn*-2 acyl chain in C(16):C(18)PE. The importance of this feature will become clear when we relate the structural properties of various dienoic PEs to their gel-to-liquid crystalline phase transition temperatures (*vide post*).

Based on the energy-minimized structure of the most stable C(16):C(18:2$\Delta^{9,12}$)PE rotamer just described above, the molecular structure of a given mixed-chain PE with *sn*-1 saturated/*sn*-2 *cis*-diunsaturated acyl chains, C(*X*):C(*Y*:2$\Delta^{n,n+3}$)PE, in the gel-state bilayer may be generalized to have a common yet flexible $s^-\Delta s^+ s^+\Delta s^-$ sequence in the *sn*-2 acyl chain; hence the structural characteristics underlying different dienoic C(*X*):C(*Y*:2$\Delta^{n,\ n+3}$)PEs can be described quantitatively by several structural parameters in terms of *X*, *Y*, and *n* as follows:

1. The major portion of the dienoic chain, from the point corresponding to the carbonyl carbon of the *sn*-1 acyl chain to the methyl terminus of the *sn*-2 acyl chain, can be considered to consist of two segments: the upper and lower segments (US and LS). These two segments are linked by the olefinic carbon with the largest number or C($n$ + 4), as shown in Fig. 2 *A*. In the case of C(18):C(20:2$\Delta^{11,14}$)PE, for example, the olefinic carbon atom with the largest number is C(15); the other three olefinic carbons are C(11), C(12), and C(14).

2. The *sn*-2 acyl chain is shortened by two C-C bond lengths along the long-chain axis because of the presence of methylene-interrupted *cis* double bonds. If the separation distance between the two methyl groups of the *sn*-1 and *sn*-2 acyl chains along the long molecular axis within a saturated identical-chain C(*X*):C(*X*)PE packed in the gel-state bilayer is $\Delta C_{ref}$, then the effective chain-length difference between the *sn*-1 and *sn*-2 acyl chains ($\Delta C$), in C-C bond lengths, for a mixed-chain diunsaturated C(*X*):C(*Y*:2$\Delta^{n,\ n+3}$)PE, is as follows: $\Delta C = X - Y + (\Delta C_{ref} + 2)$. The value of $\Delta C_{ref}$ can be taken to be ~1.5 C-C bond lengths (Huang et al., 1996), and this leads to $\Delta C = X - Y + 3.5$ C-C bond lengths, as illustrated in Fig. 2 *A*. Based on the value of $\Delta C$, the lengths of US and LS, in C-C bond lengths, can be related to $n$ and $Y$ as follows: LS = $Y - (n + 4)$ and US = $X - 1 - \Delta C - (Y - n - 4) = n - 0.5$. These two expressions are also illustrated in Fig. 2 *A*.

3. The transbilayer dimer of C(*X*):C(*Y*:2$\Delta^{n,\ n+3}$)PE at $T < T_m$ can be constructed from two energy-minimized monomers by aligning the *sn*-1 and *sn*-2 acyl chains of one monomer along the same lines as the *sn*-2 and *sn*-1 acyl chains of the opposing monomer, respectively. The constructed dimer is then subject to energy minimization, and the resulting structure is used to estimate the thickness of the hydrocarbon core of the gel-state bilayer, as illustrated

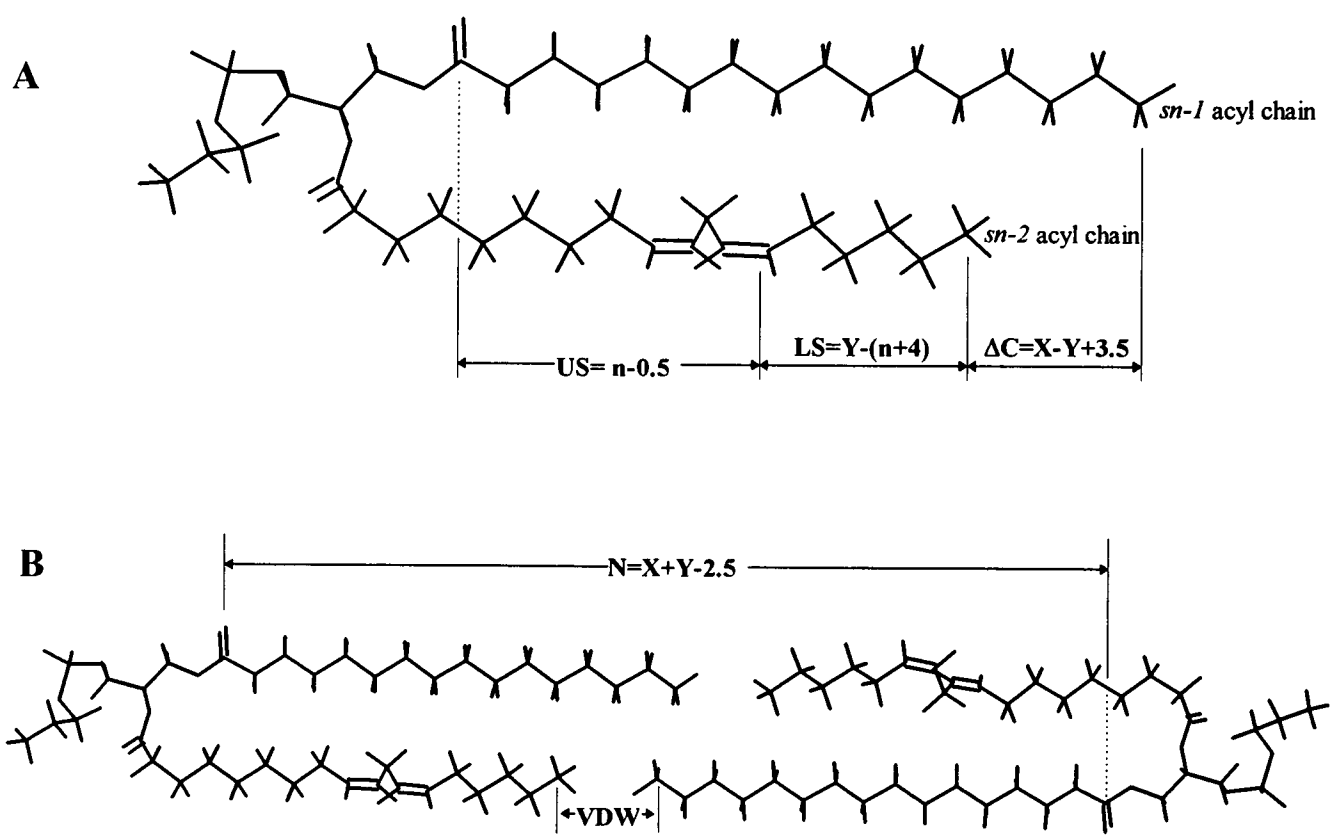


FIGURE 2 Molecular graphics drawings of the monomeric (*A*) and dimeric (*B*) structure of C(16):C(18:2$\Delta^{9,12}$)PE, illustrating the definitions of various structural parameters ($\Delta C$, LS, US, and N) in terms of *X*, *Y*, and *n*.

in Fig. 2 *B* for C(16):C(18:2$\Delta^{9,12}$)PE. The hydrocarbon core thickness of the gel-state bilayer, *N*, is the separation distance between the two carbonyl oxygens of the *sn*-1 acyl chains in the transbilayer dimer, with an orientation that is perpendicular to the bilayer surface, as depicted in Fig. 2 *B*. The *N* value, in C-C bond lengths, is related to *X* and *Y* as follows: $N = (X - 1) + \text{VDW} + (\text{US} + \text{LS}) = (X - 1) + 3.0 + n - 0.5 + Y - n - 4 = X + Y - 2.5$, where VDW is the van der Waals contact distance between the two opposing methyl groups from the *sn*-1 and *sn*-2 acyl chains (Fig. 2 *B*). Based on the MM energy-minimized structure of a transbilayer dimer, the value of VDW can be calculated to be 3 C-C bond lengths. Similar structural parameters ($\Delta C$, LS, US, and *N*) have previously been defined for monoenoic PC and PE (Huang et al., 1996). In this study, however, each of these four structural parameters is related to *X*, *Y*, and *n* in a distinctively different way. It should be mentioned that although four structural parameters ($\Delta C$, LS, US, and *N*) are presented in Fig. 2, *A* and *B*, to characterize the hydrocarbon region of the gel-state bilayer composed of dienoic $\omega$6PE, only three of them in the two sets of ($\Delta C$, LS, and *N*)/($\Delta C$, US, and *N*) are independent. One may select any three parameters in the two sets to be the independent ones. Consistent with our earlier selection of $\Delta C$, LS, and *N* as independent structural parameters in characterizing the hydrocarbon region of the bilayer composed of monoenoic lipid molecules with US > LS (Huang et al., 1996), we also select $\Delta C$, LS, and *N* as the three independent structural parameters for dienoic lipids with US > LS in the present study. In this case, the value of US is related to $\Delta C$, LS, and *N* as follows: $\text{US} = \frac{1}{2}(N - \text{VDW} - 2\text{LS} - \Delta C) = \frac{1}{2}(N - 2\text{LS} - \Delta C - 3.0)$.

## Differential scanning calorimetry studies

Fig. 3 *A* shows some representative second DSC heating curves for aqueous dispersions prepared from C(18):C(20)PE, C(18):C(20:1$\Delta^{11}$)PE, and C(18):C(20:2$\Delta^{11,\ 14}$)PE. The gel-to-liquid crystalline phase transition peak exhibited by the lipid sample is observed to downshift and broaden successively as the number of *cis* double bonds incorporated into the *sn*-2 acyl chain of the lipid molecule is increased stepwise. Specifically, the magnitude of $T_m$ decreases sharply from 79.3°C to 39.5°C as the first *cis* double bond is introduced into the *sn*-2 acyl chain between C(11) and C(12), while decreasing continuously to 18.5°C as the second *cis* double bond is incorporated into the *sn*-2 acyl chain at the methylene-interrupted position near the methyl end (Fig. 3 *B*). The transition enthalpy ($\Delta H$) is also plotted in Fig. 3 *B* as a function of the number of *cis* double bonds, which shows that like the $T_m$ value, the $\Delta H$ value decreases as the number of *cis* double bonds increases.

The phase transition behavior of a second series of C(20):C(18)PE, C(20):C(18:1$\Delta^{9}$)PE, and C(20):C(18:2$\Delta^{9,12}$)PE constituting the vesicular bilayers in the aqueous dispersion was also investigated by DSC. These lipids are the positional isomers of the first series shown in Fig. 3 *A*. As

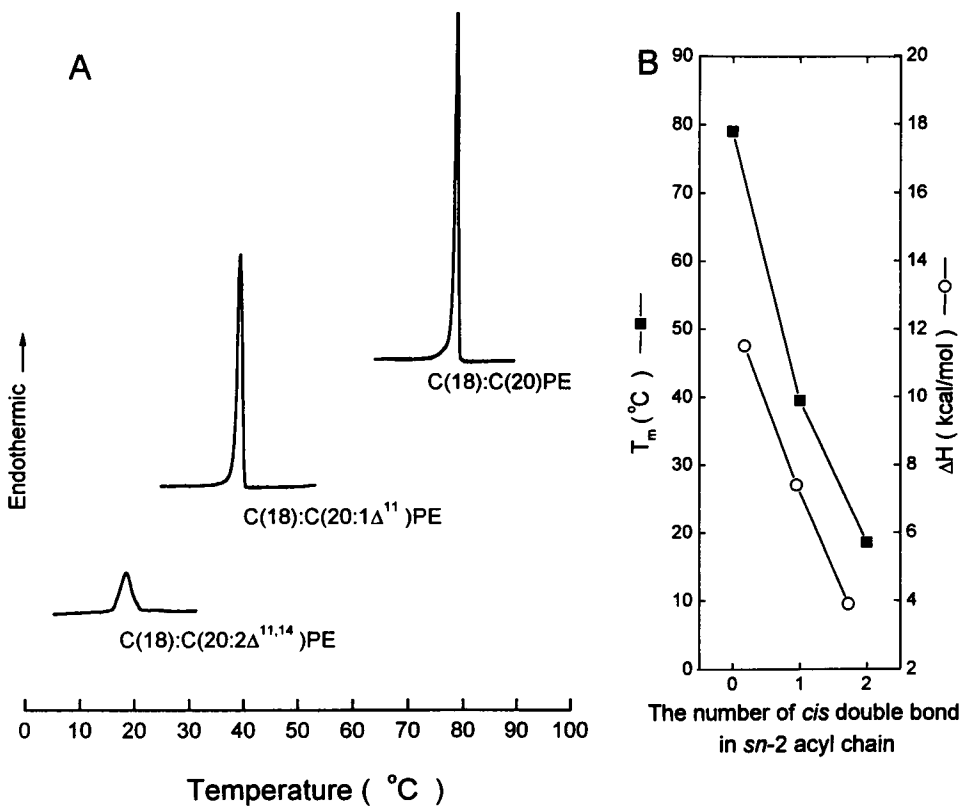


FIGURE 3 (*A*) Representative second DSC heating curves for aqueous dispersions of C(18):C(20)PE, C(18):C(20:1$\Delta^{11}$)PE, and C(18):C(20:2$\Delta^{11,14}$)PE. (*B*) The $T_m$ and $\Delta H$ values obtained from the gel-to-liquid crystalline phase transition peaks shown in *A* are plotted as a function of the number of *cis* double bonds in the *sn*-2 acyl chain.

shown in Fig. 4, *A* and *B*, a strikingly large reduction in $T_m$, from 75.8°C to 33.9°C, is discernible as the first *cis* double bond is incorporated into the *sn*-2 acyl chain between C(9) and C(10). The incorporation of a second methylene-interrupted *cis* double bond near the chain terminus further decreases the magnitude of $T_m$ down to 7.2°C. Similarly, the enthalpy change ($\Delta H$) associated with the gel-to-liquid crystalline phase transition also decreases successively as the number of *cis* double bonds in the *sn*-2 acyl chain increases stepwise from 0 to 1 and then to 2, as shown in Fig. 4 *B*.

We have further investigated calorimetrically the gel-to-liquid crystalline phase transition behavior of three series of methylene-interrupted C(*X*):C(*Y*:2ω6)PE. These three series of C(*X*):C(*Y*:2ω6)PEs are C(*X*):C(18:2$\Delta^{9,12}$)PE, C(*X*):C(20:2$\Delta^{11,14}$)PE, and C(*X*):C(22:2$\Delta^{13,16}$)PE, where the numbers of carbon atoms in the saturated *sn*-1 acyl chain, C(*X*), are 16, 18, 20, 22, and 24; hence there are 15 different lipid species in these three series of dienoic ω6PE. It should be noted that all of these ω6PEs have the same common length of LS or the lower segment of the kinked *sn*-2 acyl chain, which is 5 C-C bond lengths. To demonstrate that the bilayers composed of each of these C(*X*):C(*Y*:2ω6)PE species are able to exhibit discernibly the gel-to-liquid crystalline phase transitions, the second DSC heating scans obtained with the five different lipid species of C(*X*):C(20:2$\Delta^{11,14}$)PE are depicted in Fig. 5 as the representative ones. The thermodynamic parameters of the gel-to-liquid crystalline phase transition of the bilayers composed of these three series of dienoic ω6PE are summarized in Table 2.

## DISCUSSION

In this study, two interesting findings are observed for bilayers composed of C(*X*):C(*Y*:2ω6)PE. First it is observed that the magnitude of the gel-to-liquid crystalline phase transition temperature of the dienoic PE constituting the vesicular bilayers in the aqueous dispersion is significantly smaller than that of the saturated or monounsaturated counterpart (Figs. 3 and 4). The basis for this large $T_m$-lowering effect will be discussed initially in this section. Second, the hydrocarbon region of the bilayer prepared from each of the 15 molecular species of C(*X*):C(*Y*:2ω6)PE is characterized by three structural parameters (*N*, $\Delta C$, and LS), which are intrinsic quantities with a common unit of C-C bond lengths; however, the value of one parameter (LS) is shared by all lipid species (Table 2). Moreover, the lipid bilayer composed of a single component of C(*X*):C(*Y*:2ω6)PE displays a unique $T_m$ value (Table 2). We shall codify in this section all $T_m$ values exhibited by these 15 molecular species of C(*X*):C(*Y*:2ω6)PE in terms of their respective *N* and $\Delta C$ values, and then derive a general equation to correlate the $T_m$ value with the two structural parameters. Because the *N* and $\Delta C$ values are defined in terms of *X*, *Y*, and *n* for a given C(*X*):C(*Y*:2ω6)PE, the derived general equation can thus be used to predict the $T_m$ value for any ω6 lipid species of C(*X*):C(*Y*:2$\Delta^{n,n+3}$)PE with known *X*, *Y*, and *n* values.

Based on the experimental data shown in Figs. 3 and 4, it is evident that as a given number of *cis* double bonds is incorporated into the *sn*-2 acyl chain of PE, a considerably lower phase transition temperature ($T_m$) associated with the

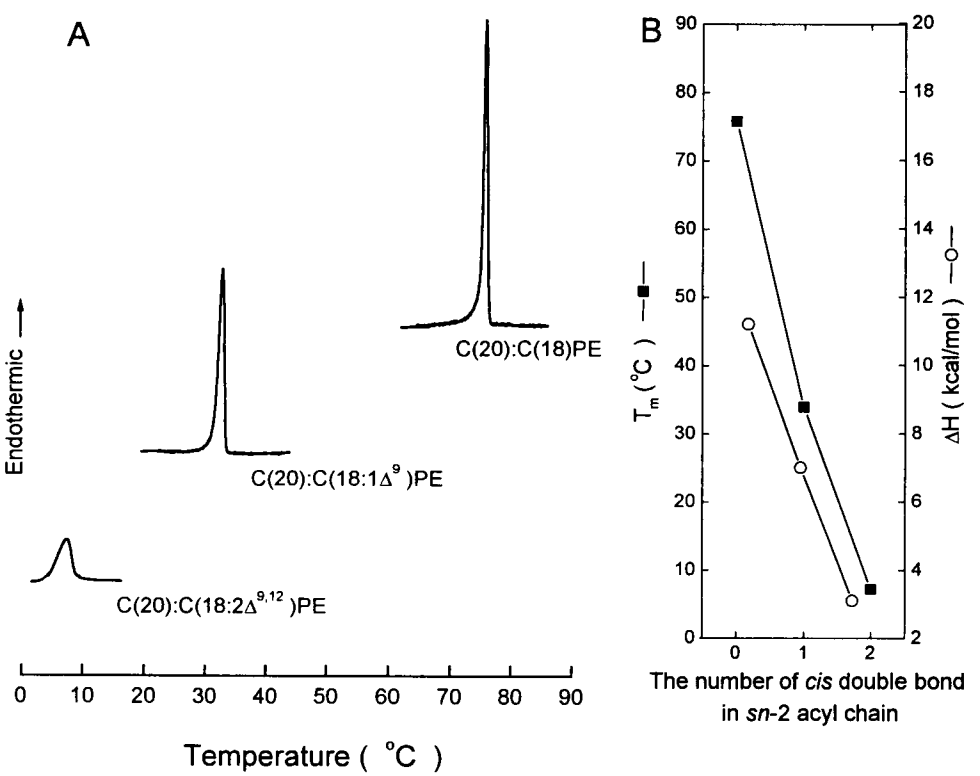


FIGURE 4 (*A*) Representative second DSC heating curves for aqueous dispersions of C(20):C(18)PE, C(20):C(18:1$\Delta^9$)PE, and C(20):C(18:$\Delta^{9,12}$)PE. (*B*) The $T_m$ and $\Delta H$ values obtained from the gel-to-liquid crystalline phase transition peaks shown in *A* are plotted against the number of *cis* double bonds in the *sn*-2 acyl chain.

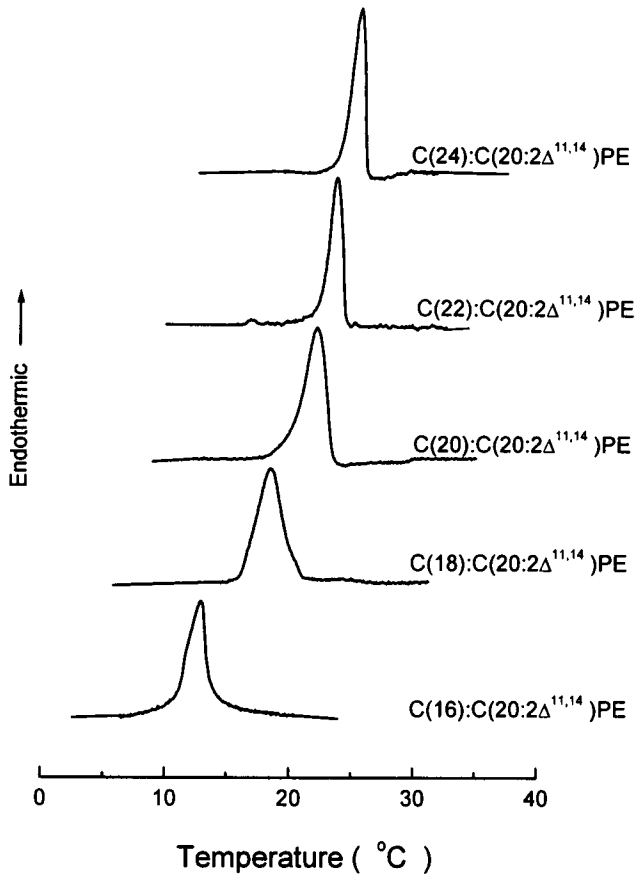


FIGURE 5 Representative second DSC heating curves of C(*X*):C(20:2$\Delta^{11,14}$)PE. It should be noted that the gel-to-liquid crystalline phase transition peak shifts upward along the temperature or *x* axis with increasing chain length in the *sn*-1 acyl chain. The values of $T_m$ and $\Delta H$ associated with these gel-to-liquid crystalline phase transition curves are summarized in Table 2.

**TABLE 2 The thermodynamic and structural parameters of C(X):C(Y:2ω6)PE**

| C(X):C(Y:2ω6)PE | *N* | US | LS | Δ*C* | $T_m^{obs}$ | Δ*H* | Δ*S* | $T_m^{cal}$ | $\Delta T_m$ |
|---|---|---|---|---|---|---|---|---|---|
| C(16):C(18:2$\Delta^{9,12}$)PE | 31.5 | 8.5 | 5 | 1.5 | −1.6 | — | — | −1.8 | 0.2 |
| C(18):C(18:2$\Delta^{9,12}$)PE | 33.5 | 8.5 | 5 | 3.5 | 4.4 | — | — | 3.3 | 1.1 |
| C(20):C(18:2$\Delta^{9,12}$)PE | 35.5 | 8.5 | 5 | 5.5 | 7.2 | ~3.1 | 11.1 | 7.2 | 0.0 |
| C(22):C(18:2$\Delta^{9,12}$)PE | 37.5 | 8.5 | 5 | 7.5 | 8.6 | ~3.5 | 12.5 | 10.0 | −1.4 |
| C(24):C(18:2$\Delta^{9,12}$)PE | 39.5 | 8.5 | 5 | 9.5 | 11.2 | ~3.9 | 13.7 | 12.1 | −0.9 |
| C(16):C(20:2$\Delta^{11,14}$)PE | 33.5 | 10.5 | 5 | −0.5 | 13.0 | 3.4 | 11.9 | 14.4 | −1.4 |
| C(18):C(20:2$\Delta^{11,14}$)PE | 35.5 | 10.5 | 5 | 1.5 | 18.5 | 3.9 | 13.4 | 18.3 | 0.2 |
| C(20):C(20:2$\Delta^{11,14}$)PE | 37.5 | 10.5 | 5 | 3.5 | 22.2 | 4.5 | 15.2 | 21.1 | 1.1 |
| C(22):C(20:2$\Delta^{11,14}$)PE | 39.5 | 10.5 | 5 | 5.5 | 23.8 | 5.0 | 16.8 | 23.2 | 0.6 |
| C(24):C(20:2$\Delta^{11,14}$)PE | 41.5 | 10.5 | 5 | 7.5 | 25.6 | 5.3 | 17.7 | 24.5 | 1.1 |
| C(16):C(22:2$\Delta^{13,16}$)PE | 35.5 | 12.5 | 5 | −2.5 | 29.6 | ~4.3 | 14.2 | 29.4 | 0.2 |
| C(18):C(22:2$\Delta^{13,16}$)PE | 37.5 | 12.5 | 5 | −0.5 | 31.5 | ~4.9 | 16.1 | 32.2 | −0.7 |
| C(20):C(22:2$\Delta^{13,16}$)PE | 39.5 | 12.5 | 5 | 1.5 | 34.3 | ~5.4 | 17.6 | 34.3 | 0.0 |
| C(22):C(22:2$\Delta^{13,16}$)PE | 41.5 | 12.5 | 5 | 3.5 | 35.7 | 5.6 | 18.1 | 35.6 | 0.1 |
| C(24):C(22:2$\Delta^{13,16}$)PE | 43.5 | 12.5 | 5 | 5.5 | 35.7 | ~5.8 | 18.9 | 36.2 | −0.5 |

*N*, US, LS, and Δ*C* are the four structural parameters described in the text; they have a common unit of carbon-carbon bond lengths. $T_m^{obs}$ and $T_m^{cal}$ are the experimentally observed and calculated gel-to-liquid crystalline phase transition temperatures in °C, respectively. Δ*H* (in kcal/mol) is the transition enthalpy obtained calorimetrically. Δ*S* (in cal/mol · K) is a calculated value obtained from the relationship $\Delta S = \Delta H/T_m^{obs}$, by assuming the transition to be a first-order transition. $\Delta T_m$ is the difference between $T_m^{obs}$ and $T_m^{cal}$.

gel-to-liquid crystalline phase transition is exhibited by the bilayer. Our MM simulation studies have shown that the presence of two methylene-interrupted *cis* double bonds in the *sn*-2 acyl chain can kink the long acyl chain and thus affects the closest lateral lipid-lipid interaction; moreover, the *sn*-2 acyl chain at $T < T_m$ is capable of fluctuating among numerous conformations with nearly identical steric energies, as shown in Table 1, because of the intrinsic flexibility of the C-C single bonds adjacent to the methylene-interrupted *cis* double bonds. Consequently, the overall lateral chain-chain contact interactions in the gel-state bilayer composed of unsaturated dienoic lipids are reduced. The decrease in $T_m$ may, therefore, be taken to reflect the loss of stabilization energy of the gel-state bilayer due to the presence of *cis* double bonds, and this loss in free energy of stabilization is most likely enthalpic. A general and very important conclusion drawn from our experimental and computational studies can be stated as follows: the marked reduction in $T_m$ after the first and the second *cis* double bonds are incorporated into the lipid's *sn*-2 acyl chain can be attributed to a stepwise increase in Gibbs free energy of the gel-state bilayer as a result of progressive weakness of the lateral chain-chain interactions.

Next we turn our attention to the experimental and computational data presented in Table 2. First, it is important to note that the LS values for all 15 lipid species under study are identical. Hence, only two independent structural parameters are needed to characterize the hydrocarbon region in the bilayer composed of each of these C(*X*):C(*Y*:2$\Delta^{n,n+3}$)PE molecules. We can further identify three sets of dienoic PE, each with a common Δ*C* value but different *N* values. Within each set, the gel-to-liquid crystalline phase transition temperature, $T_m$, increases with increasing *N*, and a linear curve with a negative slope is obtained when the $T_m$ is plotted against 1/*N* (Fig. 6 *A*). Next, we can identify another three sets of dienoic PE in Table 2, each with a constant *N* value but variable Δ*C*. A linear curve with a negative slope is also seen for each set of the identified lipids, when $T_m$ is plotted against Δ*C* (Fig. 6 *B*). Based on these linear relationships shown in Fig. 6, *A* and *B*, it is possible to formulate a general expression to correlate the $T_m$ with both structural parameters (*N* and Δ*C*) as follows:

$$T_m = a_0 - a_1(1/N) - a_2(\Delta C) \quad (1)$$

where the negative signs in the second and third terms on the right-hand side of Eq.1 reflect the negative slopes seen in the linear curves in Fig. 6, *A* and *B*. When experimental $T_m$ values and the computational data (*N*, Δ*C*) obtained with the 15 respective lipid species shown in Table 2 are substituted individually into Eq. 1, the resulting 15 simultaneous equations can be analyzed statistically by multiple regres-

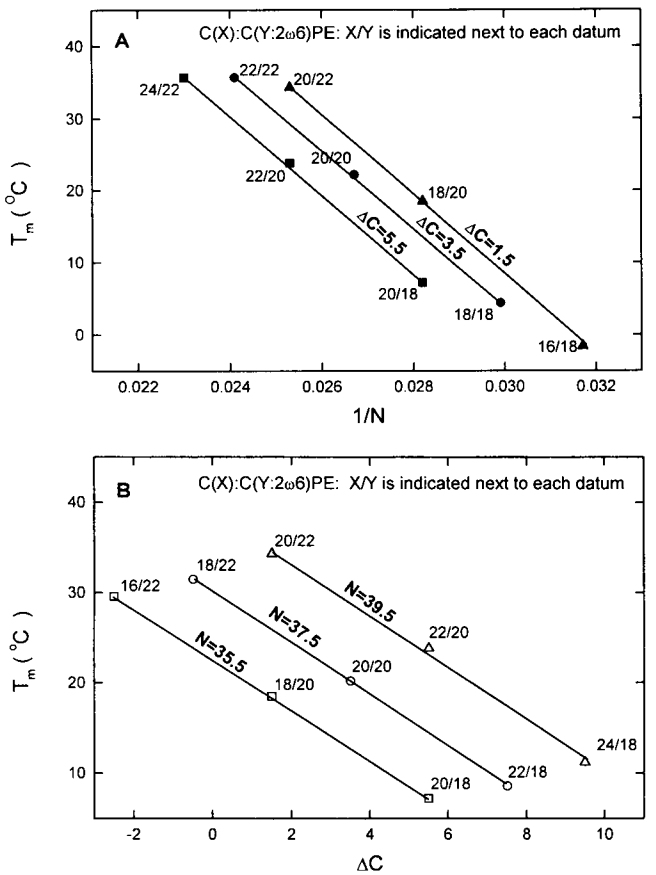


FIGURE 6 (*A*) The plot of $T_m$ versus $1/N$ for three sets of C(*X*):C(*Y*:2ω6)PE, each with a constant $\Delta C$ value. The *X* and *Y* values of C(*X*):C(*Y*:2ω6)PE are indicated as *X*/*Y* ratios next to the data points. (*B*) The plot of $T_m$ versus $\Delta C$ for three sets of C(*X*):C(*Y*:2ω6)PE, each with a constant *N* value. All of the experimental and computational data are taken from Table 2.

sion method to obtain the coefficients ($a_0$, $a_1$, and $a_2$) in Eq.1. We obtain

$$T_m = 180.48 - 5611.11\ (1/N) - 2.78\ (\Delta C) \qquad (2)$$

with a correlation coefficient of 0.9977 and a root-mean-square error of 0.8081. Based on Eq. 2, the calculated $T_m$ values for the 15 dienoic PEs under study can be generated, and they are presented in Table 2 under $T_m^{cal}$. Clearly, the value of $T_m^{cal}$ agrees well with the experimentally observed $T_m^{obs}$ value. The largest difference between $T_m^{cal}$ and $T_m^{obs}$ is 1.4°C for C(22):C(18:2$\Delta^{9,12}$)PE and C(16):C(20:2$\Delta^{11,14}$)PE, which amounts to a relative change of ~0.5% (in Kelvins).

Equation 2 is a most simple form of mathematical expression, in which the two structural parameters, *N* and $\Delta C$, are clearly seen to work against each other. Specifically, the gel-to-liquid crystalline phase transition temperature increases with increasing *N*, while decreasing as $\Delta C$ increases. Similar equations relating $T_m$ to *N* and $\Delta C$ have been derived previously for saturated and monounsaturated PC and PE (Huang et al., 1993, 1994, 1996). Taken together, these equations define a most important concept: the unique $T_m$ value of the bilayer composed of single-component phospholipids is fundamentally the net result of a delicate balance between the positive effect of *N* and the negative effect of $\Delta C$ when the third structural parameter (US or LS) is missing or invariable, and the antagonistic effect between *N* and $\Delta C$ operates regardless of the chemical nature of the lipid's headgroup.

The usefulness of Eq.2 lies in the fact that it can be employed to predict the unknown value of $T_m$ associated with the gel-to-liquid crystal line phase transition for the bilayer composed of a given species of C(*X*): C(*Y*:2ω6) PE. It is not uncommon that lipid bilayers composed of unsaturated lipids may exhibit $T_m$ values that are too low to be determined experimentally by high-resolution DSC. Equation 2 can thus be of practical use in this regard. However, it should be remembered that the predicted $T_m$ value as shown in Table 2 can have an upper-limit error of ± 1.4°C.

This work is supported, in part, by National Institutes of Health grant GM-17452.

We thank Mrs. Debbie Londeree Proffitt for her expert secretary assistance. In particular, CH acknowledges a most thoughtful discussion with Dr. Ning-sheng Huang.

## REFERENCES

Allinger, N. L., Y. H. Yuh, and J.-H. Lii. 1989. Molecular mechanics. The MM3 force field for hydrocarbons. 1. *J. Am. Chem. Soc.* 111: 8551–8566.

Applegate, K. R., and J. A. Glomset. 1991. Effect of acyl chain unsaturation on the conformation of model diacylglycerols: a computer modeling study. *J. Lipid Res.* 32:1635–1643.

Barton, P. G., and F. D. Gunstone. 1975. Hydrocarbon chain packing and molecular motion in phospholipid bilayers formed from unsaturated lecithin. *J. Biol. Chem.* 250:4470–4476.

Comfurius, P., and R. F. A. Zwall. 1977. The enzymatic synthesis of phosphatidylserine and purification by CM-cellulose column chromatography. *Biochim. Biophys. Acta.* 488:36–42.

Ernst, J., W. S. Sheldrick, and J-H. Fuhrhop. 1979. Die strukturen der essentiellen ungesättigten fettsäuren, kristallstruktur der linolsäure sowie hinweise auf die kristallstrukturen der α-linolensäure und der arachidonsäure. *Z. Naturforsch.* 34B:706–711.

Hernandez-Borrell, J., and K. M. W. Keough. 1993. Heteroacid phosphatidylcholines with different amounts of unsaturation respond differently to cholesterol. *Biochim. Biophys. Acta.* 1153:277–282.

Hitchcock, P. B., R. Mason, K. M. Thomas, and G. G. Shipley. 1974. Structural chemistry of 1,2-dilauroyl-D,L-phosphatidylethanolamine: molecular conformation and intermolecular packing of phospholipids. *Proc. Natl. Acad. Sci. USA.* 71:3036–3040.

Huang, C., S. Li, H-n. Lin, and G. Wang. 1996. On the bilayer phase transition temperatures for monoenoic phosphatidylcholines and phosphatidylethanolamines and the interconversion between them. *Arch. Biochem. Biophys.* 334:135–142.

Huang, C., S. Li, Z-q. Wang, and H-n. Lin. 1993. Dependence of the bilayer phase transition temperature on the structural parameters of phosphatidylcholines. *Lipids.* 28:365–370.

Huang, C., Z-q. Wang, H-n. Lin, E. E. Brumbaugh, and S. Li. 1994. Interconversion of bilayer phase transition temperatures between phosphatidylethanolamines and phosphatidylcholines. *Biochem. Biophys. Acta.* 1189:7–12.

Klein, R. A. 1970. The detection of oxidation in liposomes preparation. *Biochim. Biophys. Acta.* 210:486–489.

Kunau, W-H. 1976. Chemistry and biochemistry of unsaturated fatty acids. *Angew. Chem. Int. Ed. Engl.* 15:61–74.

Li, S., and C. Huang. 1996. Molecular mechanics simulation studies of dienoic hydrocarbons: from alkenes to 1-palmitoyl-2-linoleoyl-phosphatidylcholines. *J. Comp. Chem.* 17:1013–1024.

Li, S., H-n. Lin, G. Wang, and C. Huang. 1996. Effects of alcohols on the phase transition temperatures of mixed-chain phosphatidylcholins. *Biophys. J.* 70:2784–2794.

Lin, H-n., Z-q. Wang, and C. Huang. 1990. Differential scanning calorimetry study of mixed-chain phosphatidylcholines with a common molecular weight identical with diheptadecanoyl phosphatidylcholine. *Biochemistry.* 29:7063–7072.

Litman, B. J., E. N. Lewis, and I. W. Levin. 1991. Packing characteristics of highly unsaturated bilayer lipids: Raman spectroscopic studies of multilamellar phosphatidylcholine dispersions. *Biochemistry.* 30: 313–319.

MacGee, J. 1959. Enzymatic determination of polyunsaturated fatty acids. *Anal. Chem.* 31:298–302.

Mason, J. T., and F. A. Stephenson. 1990. Thermotropic properties of saturated mixed acyl phosphatidylethanolamines. *Biochemistry.* 29: 590–598.

Niebylski, C. D., and N. Salem, Jr. 1994. Calorimetric investigation of a series of mixed-chain polyunsaturated phosphatidylcholines: effects of *sn*-2 chain length and degree of unsaturation. *Biophys. J.* 67:2387–2393.

Pauling, L. 1960. The Nature of Chemical Bonds, 3rd Ed. Cornell University Press, Ithaca, NY. 138–139.

Wang, G., H-n. Lin, S. Li, and C. Huang. 1995. Phosphatidylcholines with *sn*-1 saturated and *sn*-2 *cis* monounsaturated acyl chains: their melting behavior and structures. *J. Biol. Chem.* 270:22738–22746.

Wang, Z-q., H-n. Lin, S. Li, and C. Huang. 1995. Phase transition behavior and molecular structure of monounsaturated phosphatidylcholines: calorimetric studies and molecular mechanics simulations. *J. Biol. Chem.* 270:2014–2023.

Wang, Z-q., H-n. Lin, S. Li, and C. Huang. 1994. Calorimetric studies and molecular mechanics simulations of monounsaturated phosphatidylethanolamine bilayers. *J. Biol. Chem.* 269:23491–23499.

Xu, H., F. A. Stephenson, H. Lin, and C. Huang. 1988. Phase metastability and supercooled metastable state of diundecanoyl phosphatidylethanolamine bilayers. *Biochim. Biophys. Acta.* 943:63–75.